American Journal of Materials Science and Application
2016; 4(2): 11-17
http://www.openscienceonline.com/journal/ajmsa
ISSN: 2381-6074 (Print); ISSN: 2381-6090 (Online)

Investigation of the Effect of Zn Ions Concentration on DC Conductivity and Curie Temperature of Ni-spinel Ferrite

Hussein Dawoud*, Lubna Abu Ouda, Samy Shaat*

Department of Physics, Islamic University, Gaza, Palestine

Email address

hdawoud@iugaza.edu.ps (H. Dawoud), lubna-ouda@hotmail.com (L. A. Ouda), sshaat@gmail.com (S. Shaat)
*Corresponding author

To cite this article

Hussein Dawoud, Lubna Abu Ouda, Samy Shaat. Investigation of the Effect of Zn Ions Concentration on DC Conductivity and Curie Temperature of Ni-spinel Ferrite. *American Journal of Materials Science and Application*. Vol. 4, No. 2, 2016, pp. 11-17.

Received: October 18, 2016; **Accepted**: November 3, 2016; **Published**: December 6, 2016

Abstract

The mixed polycrystalline ferrites $Ni_{1-s}Zn_sFe_2O_4$, were obtained using the standard double sintering technique by mixing high purity of metal oxides *NiO*, *ZnO* and Fe_2O_3 for different concentration of *Zn* ion. DC electric properties and inductance of the prepared samples were carried out over the temperature range of 300 up to 773 *K* using two probe method and LCR meter. The thermal dependence of DC electrical conductivity (σ_{DC}) for the mixed *Ni-Zn* spinel ferrites with different *Zn* concentrations was investigated. In general, σ_{DC} found to be increased with both increasing temperature and *Zn* content. The thermal measurement of σ_{DC} confirmed the semiconductor behavior for *Zn* substituted *Ni* spinel ferrites and follows Arrhenius relation in the investigated temperature region. The variation of σ_{DC} indicated that the conduction mechanism was correlated to a small polaron-hopping. The activation energies of both regions, ferrimagnetic (E_f) and paramagnetic (E_p) and $\Delta E=E_p-E_f$ for all studied compositions were estimated. The calculated activation energy in the ferrimagnetic region was found to be less than that in paramagnetic region. The influenced of increased *Zn* ions on σ_{DC} and activation energies was investigated. From these results, it is found that ΔE and σ_{DC} decrease with increasing of *Zn* content. The inductance measurements for the prepared samples show constant values at low temperature range up to Curie temperature (T_C), then the inductance decrease sharply except for $ZnFe_2O_4$ which confirmed that it is a paramagnetic at room temperature. The Curie temperature was determined from σ_{DC} and inductance measurement, which was found to be nearly the same and they decreased with increasing of *Zn* ions. The experimental results reveal that the electric properties and inductance, which can be dramatically changed by substitution of the non-magnetic *Zn* ions in *Ni* spinel ferrite. These improved properties of the mixed *Ni-Zn* spinel ferrite suggest uses as a soft ferrite material, which is proved an interest material for technological and scientific applications.

Keywords

Spinel Ferrite, DC Electric, Curie Temperature, Inductance, Activation Energy

1. Introduction

It is well known that the mixed of the cations of spinel ferrites in materials science has been a subject of extreme interest in recent years because of promising properties and applications. Spinel ferrites have received immense attention due to their novel magnetic, electric, optical, catalytic and dielectric properties [1-5], memory storage capacity, mechanical hardness, chemical and thermal stability, easy to synthesize and reasonable costs [5-9].

Especially, due to their interesting electrical properties they have a wide extended applications encompass an impressive in different fields [10, 11]. The electrical properties of spinel ferrites are sensitive to their composition and their structure, which in turn are sensitive to their processing conditions. The electrical conductivity of spinel ferrites is prime importance as it gives valuable information about the conduction mechanism [12].

Spinel ferrites have a general structure formula DFe_2O_4 (D is divalent metal ions) [13-15]. Among the spinel structures, nickel ferrite have been widely used in different kinds of magnetic devices, such as inductors, magnetic heads, and magnetic devices, such as inductors, magnetic heads, magnetic refrigeration and magnetic resonance imaging. Thus, the electric properties of nickel ferrite have been researched and improved [12]. *Zn*-containing ferrites form an interesting group of ferrites because of their typical electrical properties and change in a crystal structure. *Ni-Zn* ferrites are low cost materials and have important electrical properties for technological applications. Therefore, a systematic study of the electrical conductivity of the mixed *Ni-Zn* ferrite system from room temperature to well beyond Curie temperature was undertaken. The results of such a study presented in this communication are explained on the basis of the hopping model.

2. Experimental

2.1. Synthetization Samples

The mixed polycrystalline ferrites $Ni_{1-s}Zn_sFe_2O_4$, where s is the percentage increment of *Zn* ions on the compound which have the value $0.0 \le s \le 1.0$, were prepared by using the standard double sintering SSR by mixing pure metal oxides in the calculated proportions according to the formula

$$(1-s)NiO + sZnO + Fe_2O_3 \rightarrow Ni_{1-s}Zn_sFe_2O_4 \tag{1}$$

25.0 grams from high purity metal oxides were used to prepare each composition of the investigated polycrystalline spinel ferrites. The metal oxides were weighted using a sensitive electric balance (ADAM model PW124) with an accuracy $1\times10^{-4}\,gm$. The weighted metal oxides were mixed and then grounded to a very fine powder for 5 hr's. The mixed powder of metal oxides was pre-sintered at $750\,^{o}C$ for 3 hr's soaking time using a laboratory Furnace (BIFATHERM model AC62). Then the prefired powder was well ground for 3 hr's and pressed with a hydraulic press under constant pressure of 3×10^{8} pa, by using a small quantity of butyl alcohol as a binding material. Some samples were pressed in a disc shape with a diameter 11 mm and thickness (4-6) mm to measure resistance for all samples. Other samples were pressed in toroidal shape with an external radius R_o of 9.3 mm, and internal radius R_i of 4.7 mm with thickness (4-5) mm, for measuring inductance. After that, all samples were sintered at 1200°C for soaking time of 5 hr's. After sintering process, the samples were cooled down gradually to room temperature. After that, the samples were polished to obtain uniform parallel surfaces.

2.2. Properties Mesurements

A digital multimeter temperature indicator (model 2010DMM) with resolution 1°C was connected with the thermocouple K(NiCr–NiAI) was used to measure temperature from room temperature up to 773 K.

14 turns of an insulated wire were wrapped around the toroidal samples to measure the inductance as a function of temperature. The inductance was measured directly using LCR meter model (GW- instek LCR-821), with series circuit at applied voltage of 1V and constant frequency of 20 KHz with accuracy of (0.05%).

A digital multimeter (model FLUKE -177) was used to measure the resistance of the samples from room temperature up to 773 K with step of three-degrees. The increasing of temperature was carried out gradually. The specific *DC* electrical conductivity [σ_{DC} $(\Omega m)^{-1}$] of the samples was calculated from the formula:

$$\sigma_{DC} = R^{-1}\frac{l}{A} \tag{2}$$

where, R is a resistance of the sample, l and A are the thickness and the cross –sectional area of the disc sample, respectively, which were measured by a micrometer of accuracy 0.01 *mm*.

3. Results and Discussion

3.1. Temperature-Dependent of DC Electrical Conductivity

DC electrical conductivity (σ_{DC}) is one of the useful characterization techniques to understand conductivity mechanism [16, 17]. The thermal dependence of σ_{DC} for the mixed *Ni-Zn* spinel ferrites with different *Zn* concentrations was investigated from room temperature to fit beyond the transition temperature. The variation of $\ln\sigma_{DC}$ versus the reciprocal of temperature $(10^3/T)$ is depicted in Figure 1. Figure 1 illustrates that, $\ln\sigma_{DC}$ increases continuously with the increasing of temperature. This confirms that the ferrite under investigation have the same behavior of various ferrite systems [18-22].

The electrical mechanism, the change of conductivity (σ), the activation energy (E_a) at Curie temperature (T_C) and the relation of activation energies with composition can be modeled as semiconductors, electrons hopping, small polaron and phonon induced tunneling. Small polaron formation can find in materials whose conduction electrons belong to incomplete inner (d or f) shells, which due to small electron overlap; imply to form extremely narrow bands. These polarons have low activation energy in magnetic region, while more activation energy in non-magnetic regions. The conduction mechanism of ferrites, also, depends on temperature. It is reported that, the electric conduction at lower temperature (below T_C) is due to hopping electron between Fe^{2+} and Fe^{3+} ions, whereas at a higher temperature (above T_C) is due to the hopping of polarons [23, 24]. In the hopping process, the additional electron of Fe^{2+} ion requires little energy to move to an adjacent Fe^{3+} ion on O_h sites. The change in the Fe^{2+} ion content in the spinel ferrite lattice and/or the distance between them is crucial to the intrinsic resistivity of *Ni-Zn* ferrite grains, including the intrinsic grain boundaries. If the introduction of another cation into the lattice causes a change in the valence distribution on the O_h sites, then the number of electrons potentially available for transfer will be altered. More charge carriers appear to be injected into the conduction process with increasing temperature as a result the σ_{DC} increases with increasing temperature. σ_{DC} is seen to increase much more rapidly with increasing temperature as the samples undergo a ferrimagnetic to paramagnetic transition. This behavior may be attributed to the increase in drift mobility of the charge carriers.

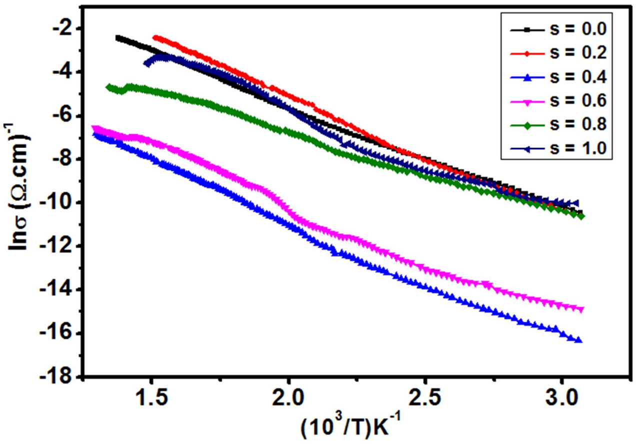

Figure 1. *Variation of* $\ln\sigma_{DC}$ *with* $(10^3/T)$ *for all prepared samples.*

Figure 2 follows Arrhenius, which presents $\ln\sigma T$ versus $(10^3/T)$, in which the values of $\ln\sigma T$ increased linearly with increasing of temperature up to T_C at which a slope changed. Several researchers for different ferrite systems [25, 26] reported similar behavior. It was proved theoretically that at T_C a change must occur in the gradient of the straight line and the magnitude of the change depends on the exchange interaction between the outer and the inner electrons, which alter T_C. Generally, the change of slope is attributed to change in conductivity mechanism. The dependence of the *DC* electrical conductivity on temperature, which is demonstrated in the Figure 2 fulfills the Arrhenius relation [27]

$$\sigma = \frac{S}{T} e^{(-E_a/kT)} \tag{3}$$

where S is a constant given by ($ne^2d^2\nu/k$), n is the number of the charge carriers, e is the electron charge, d is the distance between the nearest neighbor cations, ν is the frequency of the vibration of the crystal lattice, k is the Boltzmann constant and E_a is the activation energy.

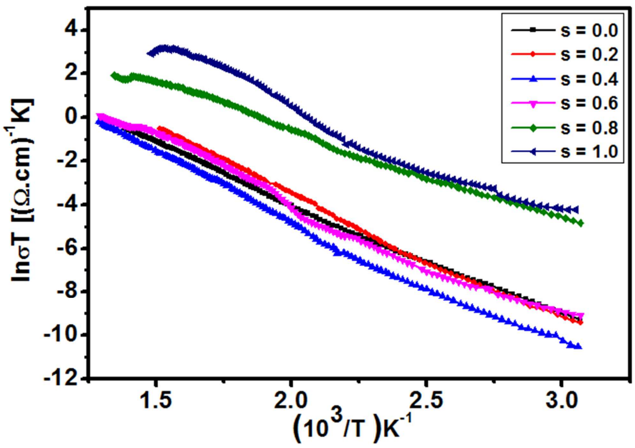

Figure 2. *Variation of* $\ln\sigma T$ *with* $(10^3/T)$ *for the samples with different compositions.*

3.2. Composition Dependent of Activation Energy

Depending on the equation (3), the activation energies of both regions ferrimagnetic (E_f) and paramagnetic (E_p) for the studied compositions were calculated using the two slopes in the Figure 2. The activation energies E_f, E_p and $\Delta E = E_p - E_f$ for the given ferrite system were plotted in Figure 3. As showing in Figure 3, with increasing of *Zn* ions concentration E_f is decreased where E_p and ΔE are increased. The increasing of activation energy is related to the increasing of the conductivity of the samples [28,29]. It is noticed that, the values of E_p are greater than of the values of E_f. In addition, from Figure 3, it is clear that, the ΔE increases with increasing of *Zn* ions in the matrix. This may be attributed to the existence of small number of oxygen vacancies [12]. It may be justified due to the increase in σ_{DC} with the increase in *Zn* ions because activation energy behaves in the similar way as that of σ_{DC} as reported by others [12]. Kadam et. al. [30] reported that, if substituted ions occupy T_d sites without disturbing O_h site, then E_a almost remains unaltered, whereas if substituted ions occupy O_h sites then the effect on E_a is greater [30]. It is reported that, hopping between ions of same metals on O_h site needs lower value of E_a than for ions of different metal [30]. The values of activation energies E_f and E_p are greater than 0.31 eV while the transition energy between Fe^{2+} and Fe^{3+} is 0.2 eV [31]. Sattar [31] suggested that if, E_a is lower than 0.2 eV then the conduction mechanism is predominantly due to the electron hopping than small polaron. Thus; our results support the small polaron hopping mechanism [32].

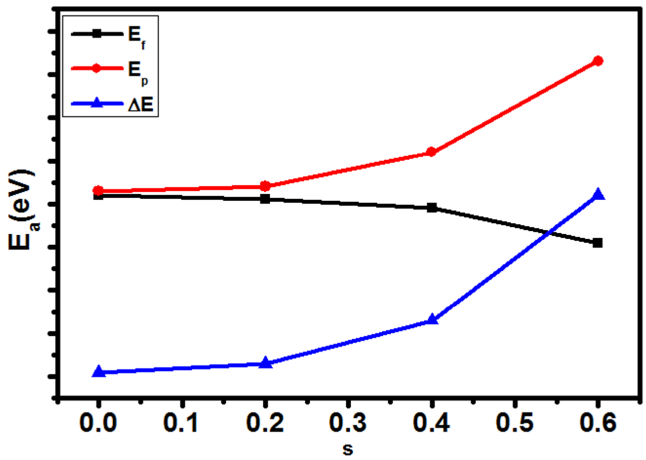

Figure 3. E_f , E_p *and* $\Delta E = E_p - E_f$ *with changing of Zn ions concentration.*

3.3. Composition Dependence of DC Electrical Conductivity

The electric conductivity in the ferrites associates with the presence of the ions for the same element in more than one valence state; these ions are distributed over the crystallographically inequivalent sites, herein T_d and O_h [33]. In line with, the cations distribution is important to explain the electrical conduction mechanism. Herein, the cations distribution of *Ni-Zn* ferrite is expected to be [34]

$$\left(Zn_s^{2+}Fe_{1-s}^{3+}\right)_{Tet.}\left\{Ni_{1-s}^{2+}Fe_{1+s}^{3+}\right\}_{Oct.}O_4^{2-} \quad (4)$$

According to the given cations distribution in (4), the change of the electrical conductivity with increasing of the *Zn* ions is explained for the mixed *Ni-Zn* spinel ferrite. It is obviously from formula (4) that, with increasing of the *Zn* ions in T_d sites implies to decrease the *Ni* ions and the Fe^{3+} ions in the T_d sites. This may be disturb the bond $Fe^{2+}-O^{2-}$ of T_d and O_h sites in the spinel lattice [24]. The $Fe^{2+}-O^{2-}$ bond exerted by the Fe^{2+} ions that is formed in the samples during the sintering process. Noting that, the sintering process effects on the number of the Fe^{2+} ions in each site. On the other hand, the electronic distribution of the $Fe^{2+}-O^{2-}$ bond is greatly affected when the *Zn* ions are increased.

For the sample with$s=0.0$, which is completely inverse spinel structure, the cations distribution in (4) becomes

$$(Fe^{3+})_{Tet.}\{Ni^{2+}Fe^{3+}\}_{Oct.}O_4^{2-} \quad (5)$$

It is clearly; that the two cations, i.e. Ni^{2+} and Fe^{3+}, occupied the O_h sites is responsible for electrical conduction in nickel ferrite, which can be described as the following

$$Fe^{3+}+e^{-}\leftrightarrow Fe^{2+} \quad (6)$$

$$Ni^{2+}+h^{+}\leftrightarrow Ni^{3+} \quad (7)$$

It has been assumed that the electrons, which participate in the formula (6) exchange process, are strongly coupled to the lattice and tunnel from one site to other due to a phonon-induced transfer mechanism. From formula (6) and (7), there is a possibility to combine of (e^- and h^+) in the O_h sties. This implies to reduce the number of electrons in the O_h sites, which leads to decrease the electrical conductivity. Otherwise, for the sample with $s=1.0$, which is perfectly normal spinel structure, the cations distribution in (4) can be expressed as following

$$(Zn^{2+})_{Tet.}\{Fe_2^{3+}\}_{Oct.}O_4^{2-} \quad (8)$$

As in formula (8), only the Fe^{3+} cation occupies the O_h sites, which is responsible for electrical conduction in zinc ferrite, which can be described as in formula (6). This leads to increase the number of electrons in the O_h sites, which implies to increase the electric conductivity. In other words, the electrical conductivity increases with increasing of the *Zn* ions as shown in Figure 4.

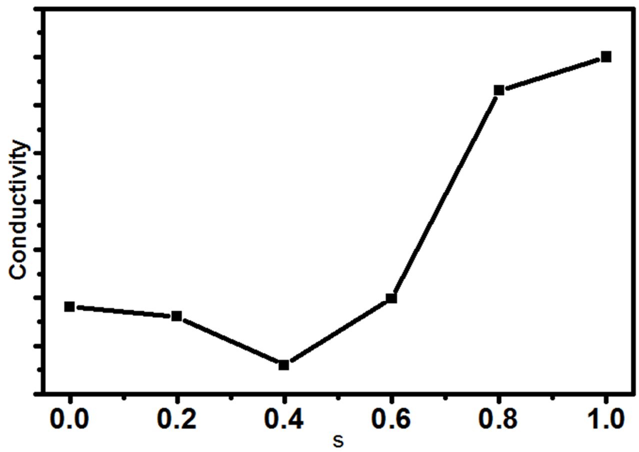

Figure 4. *Variation of conductivity with different compositions at room temperature.*

3.4. Inductance

The permeability (μ) of the ferrimagnetic materials results from the domains walls motion and spin rotational [33]. It depends upon the magnetization, the ionic structure and the degree of domain walls continuity across the grain boundary layers [35]. It is found that, μ varies with different conditions such as the soaking time, the sintering temperature, the time of sintering, the porosity, the defects introduced and atmosphere of firing due to the sintering process [33].

The relation between the inductance (L) of a closed packed coil (toroid) knitted around a substance and its permeability is given by [36, 37]:

$$\mu=\frac{2\pi L}{N^2 l\ln\left(\frac{R_o}{R_i}\right)} \quad (9)$$

where N is the number of turns, R_i and R_o are inner and outer radii of toroid, respectively, and l is thickness of toroid. The permeability of the substance can, also, be expressed by:

$$\mu=\mu_o\mu_r \quad (10)$$

with μ_o is the free space permeability and μ_r is the relative permeability. However, μ_r at low excitation level and constitutes the most important means for the comparison of soft magnetic materials can be defined as the initial permeability (μ_i). Therefore, an expression for the initial permeability can be derived as follows

$$\mu_i=\frac{2\pi L}{\mu_o N^2 l\ln\left(\frac{R_o}{R_i}\right)} \quad (11)$$

The magnetization (M) of a specific core material located inside the coil has the following expression [33, 38]

$$M = \chi_m H = \frac{(\mu_i - 1)}{4\pi} H \quad (12)$$

where, χ_m is the magnetic susceptibility, H is the magnetic field produced by the coil. By using equations (11) and (12), it can be found that

$$M = \frac{\left[2\pi L - \mu_o N^2 l \ln\left(\frac{R_o}{R_i}\right)\right]}{4\pi\mu_o N^2 l \ln\left(\frac{R_o}{R_i}\right)} H \quad (13)$$

$$\text{or } M = \left[\frac{L}{2\mu_o N^2 l \ln\left(\frac{R_o}{R_i}\right)} - \frac{1}{4\pi}\right] H \quad (14)$$

It is clear from equation (14) that, M is proportional to L. This means that, if M changes with temperature L also changes. Therefore, the transition or Curie temperature can be indicated from the variation of L with temperature. The thermal spectra of L-T curve can be taken as a test function of homogeneity of the ionic structure of the sample [35]. It depends strongly on the preparation conditions, since; these ferrites are in polycrystalline form [33]. Inductive sensing is based on measuring the variation of L for the toroidal shape for all prepared samples of mixed *Ni-Zn* ferrites. Figures 5 and 6 depict the variation of L versus temperture from room temperture to fit beyond T_C. It is noticed that, L is mostly constant up to transition happens at which a sharp drop of L is occurred for all sample except for s =1.0 as in Figure 6. It is easy to determine T_C for the samples of s = 0.0 up to s = 0.8. But for the sample of s = 1.0, i.e. $ZnFe_2O_4$, the transition tempeture can not be determined at room temperture, since it is reported as the diamagnetic substance as in [35, 39]. This means that the samples under investigation have transition from ferrimagntic at lower temperture " below T_C " to paramagntic at higher temperture "above T_C ". It is found that the transition tempertures decreased as the *Zn* content increased. As it was represented in Figure 3, the T_C decreased continuously with increasing of the Zn^{2+} ions. Other workers [40] also, observed the same behavior. This is attributed to the addition of the non-magnetic Zn^{2+} ions that replaced the magnetic Fe^{3+} ions at the T_d sites, thus; the number of the Fe^{3+} ions decrease at the T_d sites. This tends to decrease the strength of T_d and O_h exchange interactions of the type $Fe_T^{3+} - O^{2-} - Fe_O^{3+}$, apart from decreasing number of bonds or linkages between the magnetic ions [41].

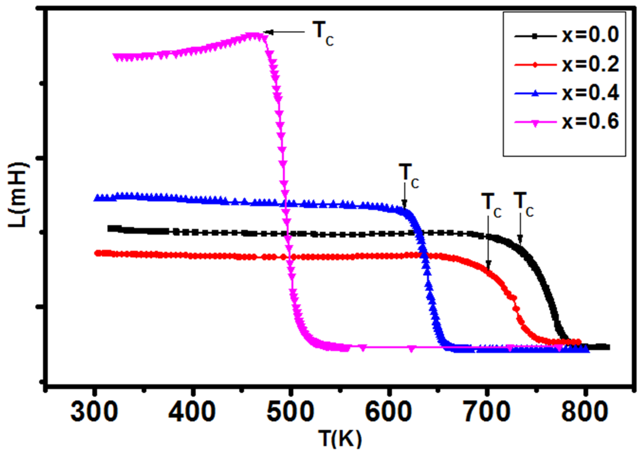

Figure 5. *Variation of L with T for the samples with s = 0.0, 0.2, 0.4 and 0.6.*

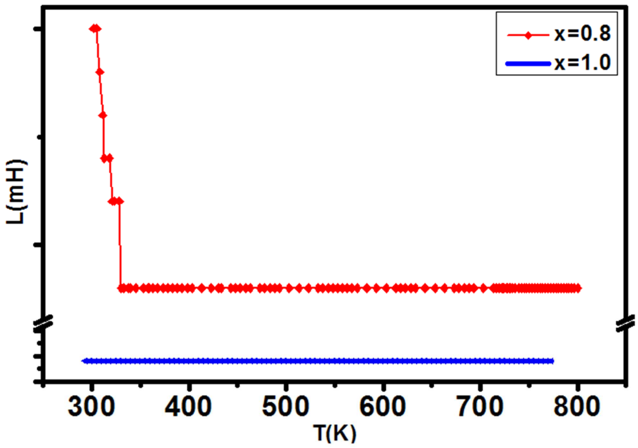

Figure 6. *Variation of L with T for the samples with s =0.8 and 1.0.*

3.5. Composition Dependence of Curie Temperature

The values of T_C for the mixed *Ni-Zn* spinel ferrite are determined from the DC electrical conductivity and the inductance measurements which are listed in Table 1. As shown in the Table 1, there is a small deviation of the T_C values from the induction and the conductivity measurements. This indicates that, the magnetic transition can be manifested in the transport property. The variation of T_C with composition s is plotted in Figure 7. From this Figure, it is noticed that T_C is decreased as s increases i.e. increasing of *Zn* ions.

Table 1. *Values of T_C which determined by induction and DC conductivity measurements for the mixed Ni-Zn spinel ferrite.*

s	Induction Results	DC conductivity Results
	$T_C(K)$	$T_C(K)$
0.0	694	666
0.2	658	641
0.4	619	624
0.6	468	458
0.8	302	-
1.0	-	-

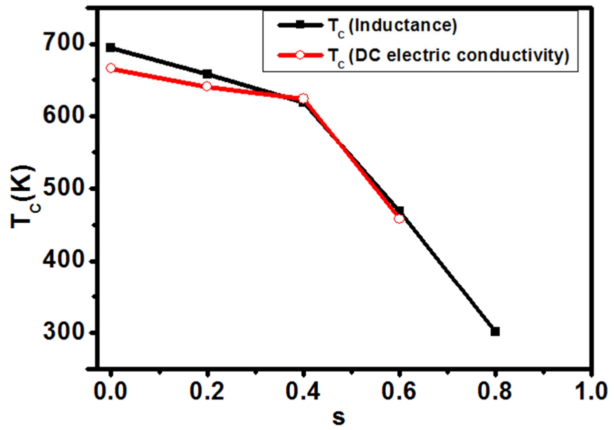

Figure 7. *Variation of T_C with Zn ratio s*

4. Conclusions

Substitution of the non-magnetic *Zn* ions in *Ni* spinel ferrite has a tremendous influence on the electrical properties. From this study, we concluded that:

- DC conductivity exhibits an excellent behavior of semiconductor materials.
- The activation energy in paramagnetic region is greater than ferrimagnetic region, which attributed to the existence of small polaron-hopping.
- The inductance can be used to determine the Curie point temperature, which showed decreasing with increasing of *Zn* ions.
- It is found that transition occurs for all samples except the sample with s = 1.0 there is no transition, so it considered as a paramagnetic at room temperature.

Furthermore, *Zn* content has significant influence on the electric properties, for *Ni*-spinel ferrites; so, the mixed *Ni-Zn* spinel ferrite is considered a soft ferrite material, which is proved an interest material for technological and scientific applications.

References

[1] S. S. Khot, N. S. Shinde, B. Ladgaonkar, B. B. Kale and S. C. Watawe, IJAET, 2011, 1(4) 422-429.

[2] B. Suryanarayana, K. C. Mouli, V. Raghavendra and B. B. Parvateesam, IJRPB, 2014,1, 92-94.

[3] K. M. Batoo and M. S. Ansari, Nanoscale Res. Lett., 7(112) (2012) 2-14.

[4] D. Carta, M. F. Casula, A. Falqui, D. Loche, G. Mountjoy, C. Sangregorio and A. Corrias, J. Phys. Chem. C, 2009, 113, 8606–8615.

[5] S. Singh, M. Singh, N. K. Ralhan, R. K. Kotnala, K. C. Verma, Adv. Mat. Lett., 2012, 3(6), 504-506.

[6] A. Mahmud, S. Islam and S. S. Nahar, IJAMSE, 5(1) (2016) 1-10.

[7] M. Shahjahan, N. A. Ahmed, S. N. Rahman1, S. Islam1 and N. Khatun, IJETCAS, 2014, 13(104), 20-25.

[8] T. Yang, R. N. C. Brown, L. C. Kempel and P. Kofinas, J Nanopart Res, 2010, 12, 2967–2978.

[9] N. Yahya, A. S. M. N. Aripin, A. A. Aziz, H. Daud, H. M. Zaid, L. K. Pah and N. Maarof, AJEAS, 2008, 1(1), 53-56.

[10] V. K. Vagolu, K. Samatha, K. C. Mouli, J. N. Kiran and P. D. Sanasi, Int J Pharm Bio Sci., 2014, 5(3), 159–175.

[11] B. P. RAO, A. M. Kumar, K. H. Rao, Y. L. N. Murthy, O. F. Caltun, I. Dumitru and L. Spinu, J OPTOELECTRON ADV M, 2006, 8(5), 1703-1705.

[12] K. Vijaya Kumar, Rapolu Sridhar, D. Ravinder and K. Rama Krishna, IJAPM, 2014, 4(2), 113-117.

[13] S. K. K. Shaat, H. C. Swart and O. M. Ntwaebborwa1 SA Institute of Physics, 2013, ISBN: 978-0-620-62819-8.

[14] S. K. K. Shaat, H. C. Swart and O. M. Ntwaeaborwa, J. Alloys Compd., 2014, 587, 600–605.

[15] S. K. K. Shaat, H. C. Swart and O. M. Ntwaeaborwa, J. Electron. Spectrosc. Relat. Phenom., 2014, 197, 72–79.

[16] S. W. Lee and C. S. Kin, J. Magn. Magn. Mater., 304(1) (2006) e418-e420.

[17] E. F. Westrum, J. R. and D. M. Grimes, J. Phys. Chem. Solids, 1957, 3, 44-49.

[18] K. R. Krishna, K. V. Kumar and D. Ravinder, AMPC, 2012, 2, 185-191.

[19] D. Ravinder and A. V. R. Reddy, Mat. Lett., 1999, 38, 265-269.

[20] A. L. Eatah, A. A. Ghani, M. F. El-Shahat and E. El Faramawy, Phys. State Sol. A, 1987, 104, 793-797.

[21] A. T. Eatah, A. A. Ghani and E. E. Earanaway, Phys. State Sol. (a), 1988, 105, 231-233.

[22] S. H. Patil, S. I. Patil, S. M. Kadam and B. K. Chougule, Czech J Phys., 42 (1992) 939-945.

[23] M. I. Rlinger and A. A. Samokhvalov, Phys. Status Solidi (b), 1977, 79(1), 9-48.

[24] K. V. Kumar, D. Ravinder, Int J Inorg Mater, 2001, 3(7), 661-666.

[25] L. I. Rabinkin, Z. I. Novikova, Ferrites. Doklady Akademii Nauk SSSR, Minsk, USSR, 1960, 146.

[26] M. Pal, P. Brahma, D. Chakravorty, J. Magn. Magn. Mater., 1996, 152(3), 370-374.

[27] K. R. Krishna, K. V. Kumar, D. Ravinder, Adv.Mater.Phys.Chem., 2012, 2, 185-191.

[28] R. R. Heikes and W. D. Johnston, J. Chem. Phys., 1957, 26(3), 582 587, http://dx.doi.org/10.1063/1.1743350.

[29] M. E. Shabasgy, J. Magn. Magn. Mater., 1997, 172, 188-192.

[30] G. B. Kadam, S. B. Shelke and K. M. Jadhav, J Electron Electr Eng., 2010, 1(1), 03-11.

[31] A. A. Sattar, Egypt. J. Sol., 2003, 26(2), 133-120.

[32] D. L. Sekulic, Z. Z. Lazarevic, M. V. Sataric, C. D. Jovalekic and N. Z. Romcevic, J Mater Sci: Mater Electron, 2015, 26, 1291–1303.

[33] S. K. K. Shaath, Advanced Ferrite Technology, LAMBART Academic Publishing, 2012.

[34] H. Dawoud, L. A-Ouda and S K. K Shaat, Chem. Sci. Trans., 2016, To be published, http://www.e-journals.in/login/accepted_articles.asp.

[35] H. A. Dawoud and S.K.K. Shaat, The Islamic University Journal, 2006, 114, 165-182.

[36] M. N. Akhtar, N. Yahya, P. B. Hussain, IJBAS-IJENS, 2009, 09(09), 37-40.

[37] M S Jebeli and N M B Mohamed, IJMSI, 2013, 1(1), 45-53.

[38] G. Nabiyouni, M. J. Fesharaki, M. Mozafari, J. Amighian, CHIN. PHYS. LETT., 2010, 27(12), 126401-126404.

[39] D. Ravinder, Mat. Lett. , 2000, 43, 129-138.

[40] H. H. Joshi and R. G. Kulkarni, J. Mater. Sci., 1986, 21, 2138-2142.

[41] M. A. Gilleo. Phys. Rev, 1958, 109, 777-781.